JOURNAL OF PROPULSION AND POWER
Vol. 11, No. 6, November–December 1995

Assumed and Evolution Probability Density Functions in Supersonic Turbulent Combustion Calculations

R. A. Baurle*
North Carolina State University, Raleigh, North Carolina 27695-7910
A. T. Hsu†
NYMA, Inc., Cleveland, Ohio 44142
and
H. A. Hassan‡
North Carolina State University, Raleigh, North Carolina 27695-7910

The objective of this investigation is to compare the use of assumed probability density function (PDF) approaches for modeling supersonic turbulent reacting flowfields with the more elaborate approach where the PDF evolution equation is solved. Previous calculations using assumed PDFs have shown modest improvements in the prediction of mean flow variables when compared with experimental data. However, these PDFs were unable to predict the higher order correlations with any reasonable degree of accuracy. Solving the evolution equation for the PDF did show slight improvements in these correlations when compared with experiment, but at a substantial cost in computer storage and time. Both approaches yielded comparable mean flow quantities.

Nomenclature

C_p = specific heat at constant pressure
D = diffusion coefficient
h = specific sensible enthalpy
k = turbulent kinetic energy
k_f, k_b = forward and backward reaction rates
Pr = Prandtl number
p = pressure
$\mathcal{P}$ = probability density function
q_j = heat flux vector
T = temperature
u_j = velocity
W_k = species molecular weights
X_k = species mole fractions
Y_k = species mass fractions
Γ = gamma function
$\Delta h^0_{f,k}$ = specific species heat of formation
δ = Dirac delta function
ν', ν'' = stoichiometric coefficients
ρ = density
σ_Y = species mass fraction variance sum
τ = turbulent time scale
Φ = dissipation function
ϕ = equivalence ratio
ψ_k = sample space variables

Introduction

IN order to obtain accurate predictions for turbulent reacting flowfields, the effect of turbulence on the chemical source terms must be addressed. The averaging of these source terms using conventional turbulence modeling is extremely difficult due to the highly nonlinear nature of these terms. An attractive option for obtaining these averages is to utilize probability density function (PDF) models that can be used to obtain averages for functions of any form. These PDF approaches consist of two types. The first being the assumed PDF approach where the form of the PDF is assumed and completely defined knowing only the first couple of moments. The second type consists of solving an evolution equation for the PDF, which is more elaborate but computationally expensive.

Many assumed forms for PDFs have been used for obtaining averages for the chemical source terms in supersonic reacting flows. All of these forms have either neglected the effects of composition fluctuations or assumed statistical independence between the temperature and the composition. Frankel et al.[1] examined the effects of temperature fluctuations on the chemical source terms using both Gaussian and beta forms for the PDF. Both assumed forms yielded similar results and showed modest improvements in the mean flow properties over treating these source terms in a laminar fashion when compared to experiment. Later Narayan and Girimaji[2] combined a moment method to account for temperature fluctuations with a multivariate β distribution developed by Girimaji[3] to account for composition fluctuations. Their results showed the effect of the multivariate β distribution to be minimal on the mean flow variables. This same behavior was seen later by Baurle et al.[4]

The use of evolution PDF methods for low-speed turbulent reacting flows has been examined extensively.[5–7] However, until recently,[8,9] the extension of these methods to high-speed flows has been practically nonexistent due to difficulties arising from shocks and strong dilatation terms. Hsu et al.[8,9] solved the evolution equation for the joint PDF of specific enthalpy and mass fractions in conjunction with a computational fluid dynamics (CFD) flow solver for the Reynolds-averaged Navier–Stokes equations. Significant improvements over calculations without the PDF were noted when compared to experimental data for high-speed reacting flows. Simplistic kinetic models[8,9] were used because of the extensive CPU requirements for the solution of the PDF evolution equation. Moreover, no comparisons with solutions using assumed PDF approaches were attempted.

Presented as Paper 94-3180 at the AIAA/ASME/SAE/ASEE 30th Joint Propulsion Conference, Indianapolis, IN, June 27–29, 1994; received July 20, 1994; revision received Jan. 26, 1995; accepted for publication Jan. 26, 1995.

*Research Assistant, Mechanical and Aerospace Engineering. Student Member AIAA.
†Supervisor, Computational Physics Section; currently Engineer, Allison Engine Co., Indianapolis, IN 46206. Member AIAA.
‡Professor, Mechanical and Aerospace Engineering. Associate Fellow AIAA.

The present work utilizes a full chemistry model to accurately describe the chemical kinetics of the flow and the results of both PDF approaches are compared with experiment. Two axisymmetric, reacting free shear flows are examined in this work. The first case studied was the coaxial jet experiment conducted by Beach et al.[10] In this experiment only mean flow variables were measured. The second case is a more recent experiment conducted by Cheng et al.,[11] where both mean quantities and rms values of the fluctuating components were measured using uv Raman scattering and laser-induced predissociative fluorescence techniques. These additional measurements of rms quantities provide an excellent test base for evaluating the PDF models.

Assumed PDF Approach

For the assumed PDF approach, the species continuity equations are solved in conjunction with the Reynolds-averaged Navier–Stokes equations. To obtain the average of the chemical source terms $\dot{\omega}_k$ that appear in the species equations, i.e.,

$$\dot{\omega}_k = W_k \sum_{l=1}^{nr} (\nu''_{kl} - \nu'_{kl}) \left[k_{f_l}(T) \prod_{m=1}^{ns} \left(\frac{\rho_m}{W_m}\right)^{\nu'_{ml}} - k_{b_l}(T) \prod_{m=1}^{ns} \left(\frac{\rho_m}{W_m}\right)^{\nu''_{ml}} \right] \tag{1}$$

a joint PDF of temperature and composition is needed. In this work, the joint PDF was chosen as

$$\mathcal{P}(T, \rho_k) = \delta(\rho - \bar{\rho})\mathcal{P}(T)\mathcal{P}(Y_1, \ldots, Y_{ns}) \tag{2}$$

Here, the PDF of temperature $[\mathcal{P}(T)]$ was assumed to be a Gaussian distribution

$$\mathcal{P}(T) = \frac{1}{\sqrt{2\pi\widetilde{T''^2}}} \exp\left[-\frac{(T - \tilde{T})^2}{2\widetilde{T''^2}} \right] \tag{3}$$

and the PDF of the mass fractions $[\mathcal{P}(Y_1, \ldots, Y_{ns})]$ was chosen as the multivariate β distribution developed by Girimaji[3]

$$\mathcal{P}(Y_1, \ldots, Y_{ns}) = \frac{1}{C}\left[\delta\left(1 - \sum_{k=1}^{ns} Y_k\right) \prod_{k=1}^{ns} Y_k^{\beta_k - 1} \right] \tag{4}$$

where

$$C = \frac{\prod_{k=1}^{ns} \Gamma(\beta_k)}{\Gamma\left(\sum_{k=1}^{ns} \beta_k\right)}, \qquad \beta_k = \tilde{Y}_k\left(\frac{1 - S}{\tilde{\sigma}_Y} - 1\right) \tag{5}$$

$$S = \sum_{k=1}^{ns} (\tilde{Y}_k)^2, \qquad \tilde{\sigma}_Y = \sum_{k=1}^{ns} \widetilde{Y''^2_k} \tag{6}$$

The Gaussian PDF $[\mathcal{P}(T)]$ requires knowledge of the mean temperature and the temperature variance. The mean temperature is obtained from the Reynolds-averaged Navier–Stokes equations. The temperature variance is calculated from the sensible enthalpy variance by neglecting fluctuations on the specific heat, i.e.,

$$h = C_p T \approx \bar{C}_p T, \quad \widetilde{h^2} = (\tilde{h}^2 + \widetilde{h''^2}) \approx \bar{C}_p^2(\tilde{T}^2 + \widetilde{T''^2}) \tag{7}$$

where

$$\bar{C}_p \equiv \sum_{k=1}^{ns} \tilde{Y}_k \frac{\int C_{p_k}(\tilde{T})\, \mathrm{d}\tilde{T}}{\tilde{T}} \tag{8}$$

The sensible enthalpy variance (in modeled form) is governed by

$$\frac{\partial(\bar{\rho}\widetilde{h''^2})}{\partial t} + \frac{\partial(\bar{\rho}\tilde{u}_j\widetilde{h''^2})}{\partial x_j} = \frac{\partial}{\partial x_j}\left[\left(\frac{\mu}{Pr} + \frac{\mu_t}{Pr_t}\right)\frac{\partial \widetilde{h''^2}}{\partial x_j} \right] + 2\frac{\mu_t}{Pr_t}\frac{\partial \tilde{h}}{\partial x_j}\frac{\partial \tilde{h}}{\partial x_j} - C_h\frac{\bar{\rho}\widetilde{h''^2}}{\tau} - 2\overline{h'' \sum_{k=1}^{ns} \dot{\omega}_k \Delta h^0_{f,k}} \tag{9}$$

A detailed description on the modeling of this equation is given in Ref. 12.

The multivariate β PDF $[\mathcal{P}(Y_1, \ldots, Y_{ns})]$ is completely defined given the mean mass fractions and the sum of the mass fraction variances $\tilde{\sigma}_Y$. The mean mass fractions are determined from the species continuity equations, and $\tilde{\sigma}_Y$ is governed by the model equation

$$\frac{\partial(\bar{\rho}\tilde{\sigma}_Y)}{\partial t} + \frac{\partial(\bar{\rho}\tilde{u}_j\tilde{\sigma}_Y)}{\partial x_j} = \frac{\partial}{\partial x_j}\left[\bar{\rho}(D + D_t)\frac{\partial \tilde{\sigma}_Y}{\partial x_j} \right] + 2\sum_{k=1}^{ns} \bar{\rho} D_t \frac{\partial \tilde{Y}_k}{\partial x_j}\frac{\partial \tilde{Y}_k}{\partial x_j} - C_{\sigma_Y}\frac{\bar{\rho}\tilde{\sigma}_Y}{\tau} + 2\sum_{k=1}^{ns} \overline{\dot{\omega}_k Y''_k} \tag{10}$$

Further details on the modeling of this equation are given in Ref. 12.

Evolution PDF Approach

For the evolution PDF approach, the species continuity equations are replaced by the PDF evolution equation. The single-point joint scalar PDF $[\mathcal{P}(\psi_k, x_j, t)]$ evolution equation is derived from the specific sensible enthalpy and species continuity equations. If the effect of pressure fluctuations on the density is neglected [e.g., $\rho = \rho(\bar{p}, h, Y_k)$], then this equation can be expressed as

$$\frac{\partial \tilde{\mathcal{P}}}{\partial t} + \tilde{u}_j\frac{\partial \tilde{\mathcal{P}}}{\partial x_j} + \frac{\partial(S_k\tilde{\mathcal{P}})}{\partial \psi_k} = -\frac{1}{\bar{\rho}}\frac{\partial}{\partial x_j}(\bar{\rho}\langle u''_j|\psi_m\rangle\tilde{\mathcal{P}}) + \frac{\partial}{\partial \psi_k}\left(\frac{1}{\rho}\left\langle \frac{\partial J^k_j}{\partial x_j}\middle|\psi_m\right\rangle\tilde{\mathcal{P}}\right) - \frac{\partial}{\partial \psi_{ns+1}}\left[\frac{1}{\rho}\left\langle\left(\frac{\mathrm{D}p}{\mathrm{D}t} + \Phi\right)\middle|\psi_m\right\rangle\tilde{\mathcal{P}}\right] \tag{11}$$

where

$$\psi_k = \begin{cases} \text{sample space of } Y_k, & k = 1, ns \\ \text{sample space of } h, & k = ns + 1 \end{cases}$$

$$S_k = \begin{cases} \dfrac{\dot{\omega}_k}{\rho}, & k = 1, ns \\ -\displaystyle\sum_{k=1}^{ns} \Delta h^0_{f,k}\frac{\dot{\omega}_k}{\rho}, & k = ns + 1 \end{cases} \tag{12}$$

$$J^k_j = \begin{cases} -\rho D\dfrac{\partial Y_k}{\partial x_j}, & k = 1, ns \\ q_j, & k = ns + 1 \end{cases}$$

The first two terms represent convection in the physical space. The third term represents the transport of $\tilde{\mathcal{P}}$ in the scalar space due to reaction. The terms on the right-hand side (RHS) of the previous equation require modeling. The first of these is the turbulent diffusion term that is modeled using the gradient diffusion approximation, i.e.,

$$\langle u''_j|\psi_m\rangle\tilde{\mathcal{P}} = -D_t\frac{\partial \tilde{\mathcal{P}}}{\partial x_j} \tag{13}$$

The second term on the right is the contribution due to molecular mixing and is modeled using a binary interaction model as described in Ref. 13. The final term accounts for compressibility and viscous dissipation. These terms are modeled by assuming that the velocity and pressure are statistically independent from the species mass fractions and enthalpy. This allows the conditional expectation to be replaced by the absolute expectation so that conventional turbulence modeling can be applied.

It is emphasized that Eq. (11) is not exact for high-speed flows.[14] The PDF only contains information on the composition and enthalpy that is not enough to uniquely determine the density. As a result, the pressure (or some other thermodynamic variable) must be supplied by some other means in order to compute the density. In this work, the mean pressure was supplied to the PDF evolution solver from the Navier–Stokes solver. As a result, the evaluation of the reaction term is now, strictly speaking, only an approximation.

Due to the large dimensionality of the joint PDF, solving this equation with a finite difference approach is not practical since the computational cost can be shown to rise exponentially with the dimensionality of the PDF. Instead, the previous equation is simulated using a fractional step Monte Carlo scheme as described in Ref. 15. The computational cost of this scheme rises linearly with the dimensionality of the PDF.

In an effort to minimize the number of stochastic particles necessary to simulate the PDF evolution equation, a combined ensemble/time averaging procedure was used to average the scalar properties as described in Ref. 9. For this procedure, the combined ensemble/time average of some quantity Q at iteration "n" is given by

$$\langle \bar{Q} \rangle_n = [1/(1 + G_n)][\langle Q \rangle_n + G_n \langle \bar{Q} \rangle_{n-1}] \tag{14a}$$

$$G_n = C_n(G_{n-1} + 1), \qquad G_0 \equiv 0 \tag{14b}$$

where $\langle Q \rangle$ represents a conventional ensemble average, and $\langle \bar{Q} \rangle_n$ represents the combined ensemble/time average at iteration n. The variable C_n that controls the weighting function was chosen as $\max[1 - (1/n^{0.75}), \frac{9}{10}]$. All computations were performed with 25 stochastic particles, which was found to be sufficient to yield particle number independent solutions.

Results and Discussion

All calculations were carried out using a cell-centered finite volume code developed at North Carolina State University. The numerical scheme used to integrate the Navier–Stokes equations together with the species continuity equations is described in Ref. 16. The PDF evolution equation solver was developed at the NASA Lewis Research Center and modified to accommodate general kinetic models. To alleviate the stiffness involved with the chemical source terms, the reaction step is advanced in an implicit manner. The chemistry model employed is the abridged Jachimowski[12,17] chemistry model. For all calculations, the turbulent Prandtl and Lewis numbers were set to 1, and the model constants C_h and C_{σ_Y} were set as one-half.

The molecular mixing model as mentioned previously is a binary interaction model where the extent of mixing for a given pair of stochastic particles is controlled by the parameter

$$A = C\xi(\Delta t/\tau) \tag{15}$$

Here, C is a model constant usually prescribed a value of two, ξ is a uniformly distributed random number between zero and one, and Δt is the time increment for the integration of the PDF equation. This model assumes the turbulent time scale is larger than the time increment, however, at least in some regions of the flowfield it should be of the same order as the time increment to allow molecular mixing to take place. The time increment is limited in the convection/diffusion process by the stability bound [Courant–Friedrichs–Lewy (CFL) $\leq$ 1], which is a function of the grid spacing, mean velocity, and turbulent diffusion coefficient. These quantities are independent of the turbulent time scale that varies depending on the turbulence model being used. The turbulent time scale was found to vary by as much as an order of magnitude between the turbulence models examined in this work with the smallest time scales given by the algebraic models and the largest by the two-equation turbulence models. Thus, to minimize the need to change the value of the constant C by such a large amount, the mixing parameter A was rescaled at each iteration level using the maximum value of the ratio $\Delta t/\tau$.

Table 1 Burner exit conditions (Beach)

Exit conditions	Inner jet	Outer jet
Mach number	2.0	1.9
Temperature, K	251.0	1495.0
Pressure, MPa	0.1	0.1
$\sqrt{\bar{k}}$, m/s	$0.01\|u_j\|$	$0.01\|u_j\|$
$\sqrt{\widetilde{T''2}}$, K	$0.05T$	$0.05T$
$\sqrt{\sigma_Y}$	0.0	0.05
Mass fraction		
Y_{H_2}	1.0	0.0
Y_{O_2}	0.0	0.241
Y_{N_2}	0.0	0.478
Y_{H_2O}	0.0	0.281
All others	0.0	0.0

Note: Inner jet diameter = 0.006525 m; outer jet diameter = 0.0653 m; and lip thickness = 0.0015 m.

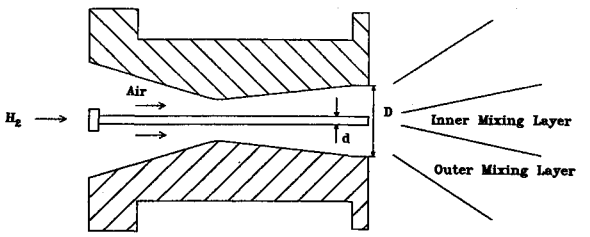

Fig. 1 Schematic diagram of flowfield.

The first case considered is the Beach coaxial experiment.[10] A schematic diagram of this flowfield is given in Fig. 1. For this case a 61 × 71 grid was used that extends 30 i.d.s downstream of the jet exit, and 2 i.d.s in the transverse direction. This calculation did not take into account any influence from the ambient air. The grid is clustered to give more resolution around the lip region in the transverse direction and more resolution near the burner exit in the streamwise direction. The nozzle exit conditions are summarized in Table 1. The fuel injector lip is assumed adiabatic and noncatalytic. All variables are extrapolated at the far-field and outflow planes, and symmetry conditions are applied at the centerline.

In an effort to examine the effects of the turbulence model on the PDF solver, calculations were performed using algebraic, one-equation, and two-equation turbulence models. The algebraic turbulence model employed was the model developed by Cohen[18] for jet flows. The implementation of the model and model constants is described in Ref. 16. The one-equation model used is based on the turbulent kinetic energy and is described in Ref. 19. Finally, the two-equation model was a k-ω model as employed in Ref. 20. The results (not included) were comparable for the most part, with the one-equation model slightly outperforming the other models. Because of this, the remainder of the results employs the one-equation turbulence model.

Figure 2 compares the mean mass fractions computed from the assumed PDF with experiment and Fig. 3 compares the results of the evolution PDF with experiment. As can be seen, both sets of calculations agree fairly well with the experiment. The use of the evolution PDF results in a slight improvement,

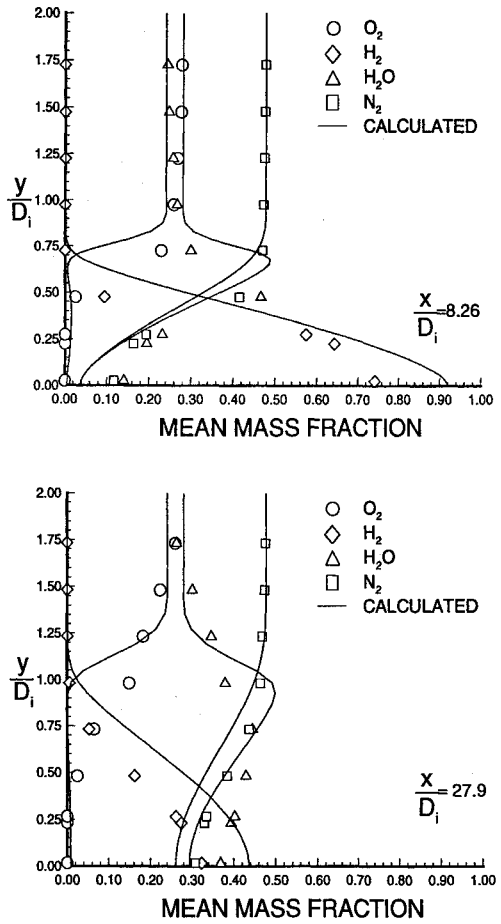

Fig. 2 Comparison of mass fraction profiles with the beach experiment (assumed PDF).

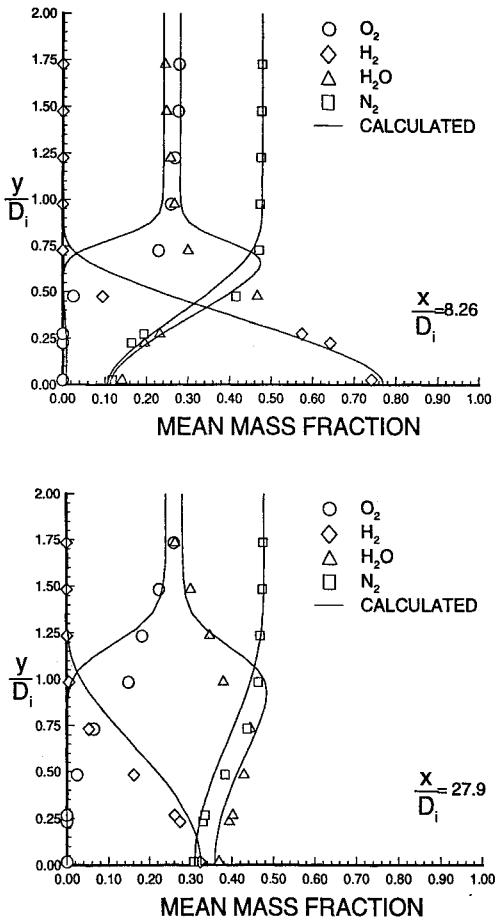

Fig. 3 Comparison of mass fraction profiles with the beach experiment (evolved PDF).

however, the cost involved for this improvement is large. The assumed PDF results required approximately 2000 CPU s on a Cray Y-MP, whereas the computations with the evolution PDF required about 9000 CPU s. This substantial cost was due mainly to the treatment of the chemical terms that had to be performed in an implicit manner to alleviate the stiffness of these terms. Approximately 80% of the simulation CPU time was spent computing the reaction phase.

For a grid resolution study, the previous results for the evolution PDF are compared with the results using a 105 × 105 grid in Fig. 4. This figure shows the two calculations to yield similar results, suggesting the solution to be grid independent.

The second case considered is the experiment conducted by Cheng et al.[11] For this case, the effects of the ambient air are taken into account, and a block grid was added to the ambient inflow region as discussed in Ref. 12. The main grid consists of 61 × 61 grid nodes, and the ambient block contains 37 × 17 nodes. The grid is clustered to give more resolution near the lip regions in the transverse direction and near the burner exit in the streamwise direction. This grid has previously been shown to adequately resolve the flowfield.[21] The burner lip surfaces are assumed adiabatic and noncatalytic. At the inner and outer jet exits the flow is turbulent, however, only the means and variances of the scalars are given from experiment. In general, this is not enough information to specify the PDF exiting the jets. As a result, the stochastic particles were assumed to be distributed according to the PDF given by Eq. (2) at the jet exit. At the ambient inflow plane the flow is subsonic so that all variables are specified except the x-velocity component that is extrapolated from the interior. All variables are extrapolated at the far-field and outflow boundaries, and symmetry conditions are enforced at the centerline. The burner exit conditions for this case are summarized in Table 2.

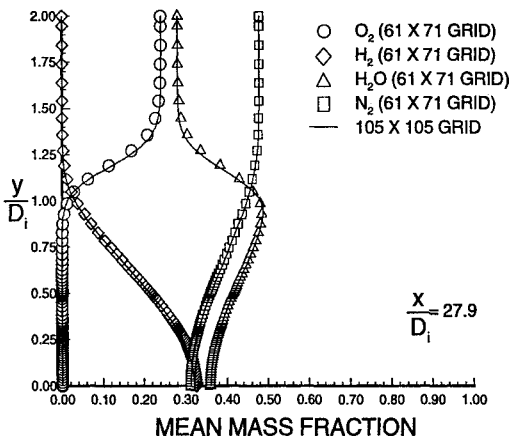

Fig. 4 Comparison of mass fraction profiles with a 61 × 71 grid and a 105 × 105 grid.

Figures 5–7 compare the mean H_2O mole fraction, OH mole fraction, and mean temperature profiles with experiment at axial stations of 1 and 4 in. downstream of the burner. The agreement with experiment is quite good for the main reaction product H_2O, and both the assumed and evolved PDF showed similar values at each station. The computed values of the minor species OH also agrees reasonably well with experiment, however, the assumed PDF is predicting the onset of combustion just after the 1-in. station as the experiment suggests, whereas the evolved PDF is predicting combustion to start somewhat closer to the 2-in. station. A pos-

Table 2 Burner exit conditions (Cheng)

Exit conditions	Inner jet	Outer jet	Ambient air
Mach number	1.0	2.0	0.0
Temperature, K	545.0	1250.0	300.0
Pressure, MPa	0.112	0.107	0.101
$\sqrt{\tilde{k}}$, m/s	$0.01\|u_j\|$	$0.01\|u_j\|$	0.0
$\sqrt{\widetilde{T''2}}$, K	125.0	125.0	0.0
$\sqrt{\sigma_Y}$	0.0	0.05	0.0
Mass fraction			
Y_{H_2}	1.0	0.0	0.0
Y_{O_2}	0.0	0.245	0.233
Y_{N_2}	0.0	0.580	0.757
Y_{H_2O}	0.0	0.175	0.01
All others	0.0	0.0	0.0

Note: Inner jet diameter = 0.002362 m; outer jet diameter = 0.01778 m; inner jet/outer jet lip thickness = 0.0007239 m; and outer jet/ambient air lip thickness = 0.0004 m.

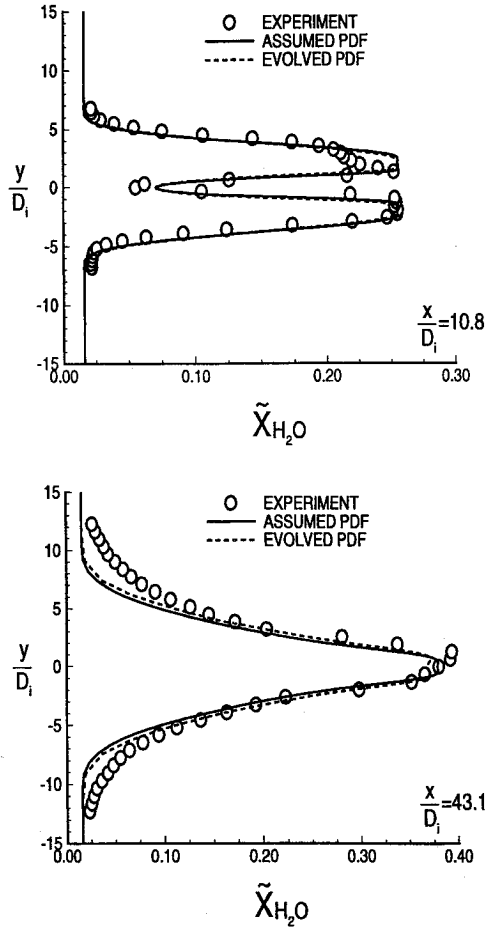

Fig. 5 Comparison of H_2O mole fraction profiles with the Cheng experiment.

sible explanation for this behavior may lie in the convection/diffusion phase of the simulation. It has been found from previous CFD calculations that too much numerical dissipation can significantly shift the ignition point farther downstream from the burner. Before the Monte Carlo simulation of convection is employed, the convective terms are discretized in a first-order upwind manner, which is known to be highly dissipative. This may explain why the evolved PDF results predict combustion farther downstream than does the assumed PDF results. Comparisons with experiment of the mean temperature are given in Fig. 7. Both the assumed and evolved PDF results are underpredicting the temperature. The assumed PDF, however, is showing significantly higher peak temperature values than the evolved PDF results.

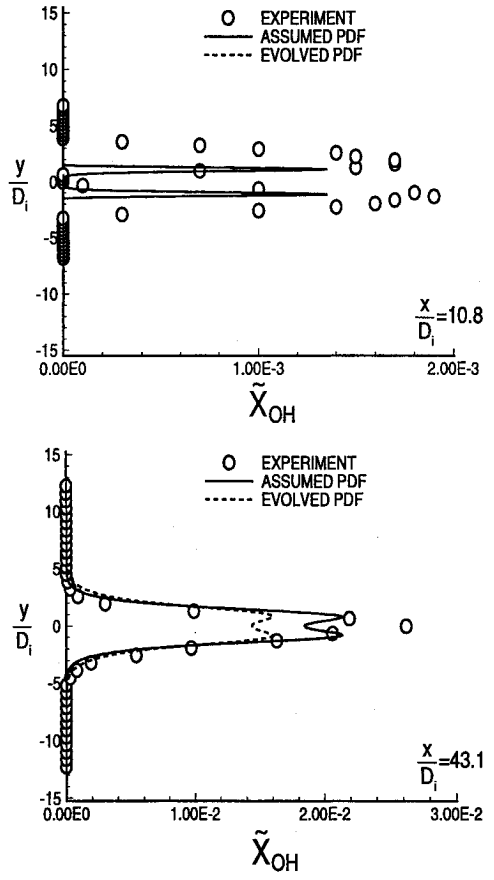

Fig. 6 Comparison of OH mole fraction profiles with the Cheng experiment.

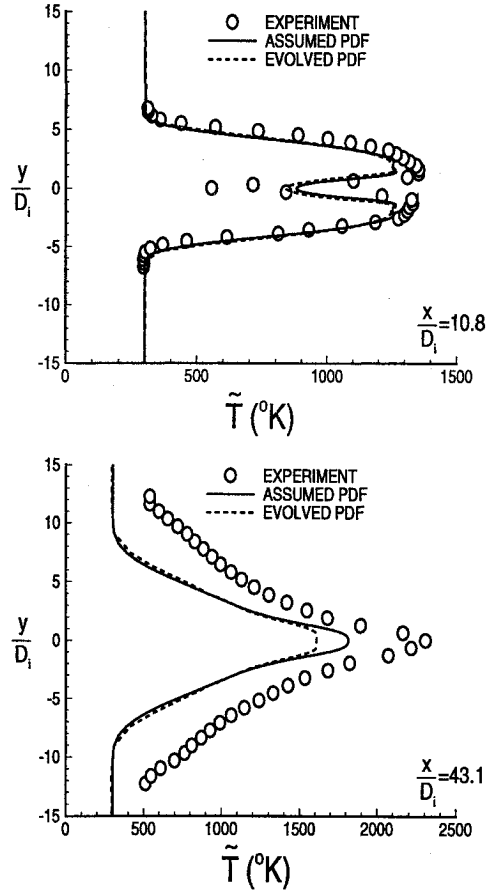

Fig. 7 Comparison of mean temperature profiles with the Cheng experiment.

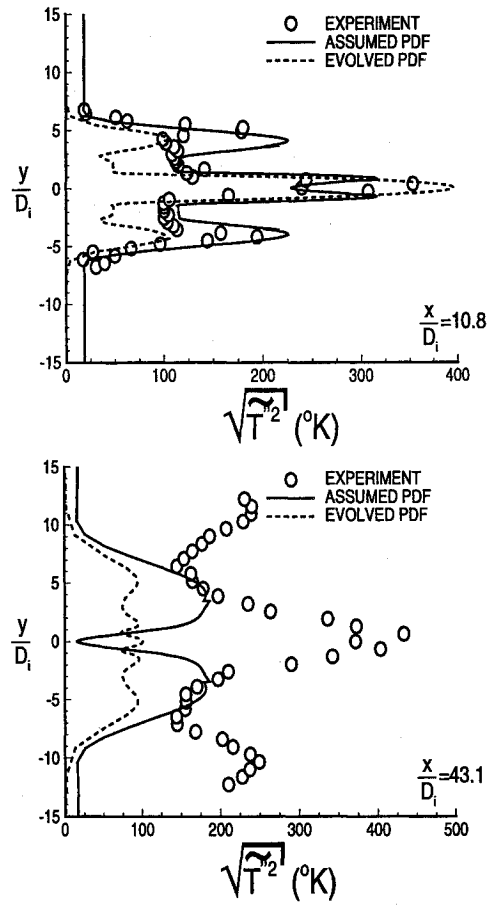

Fig. 8 Comparison of rms temperature profiles with the Cheng experiment.

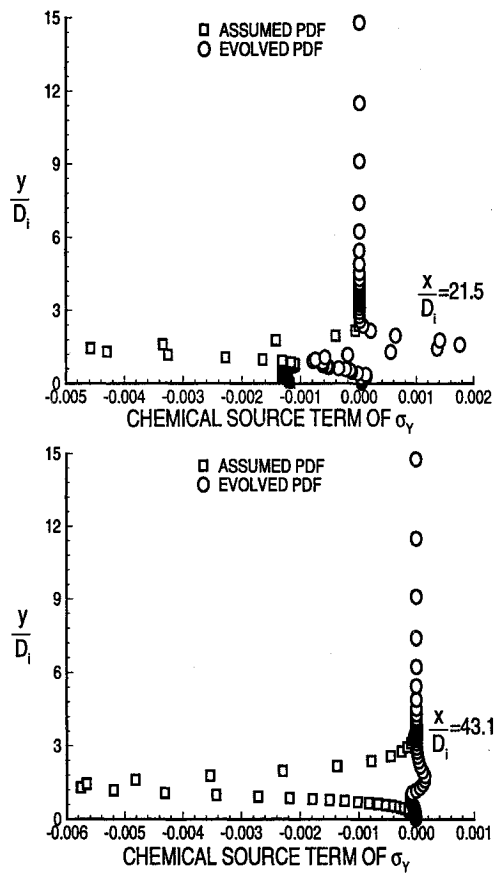

Fig. 9 Comparison of the chemical source term in the equation governing $\tilde{\sigma}_Y$.

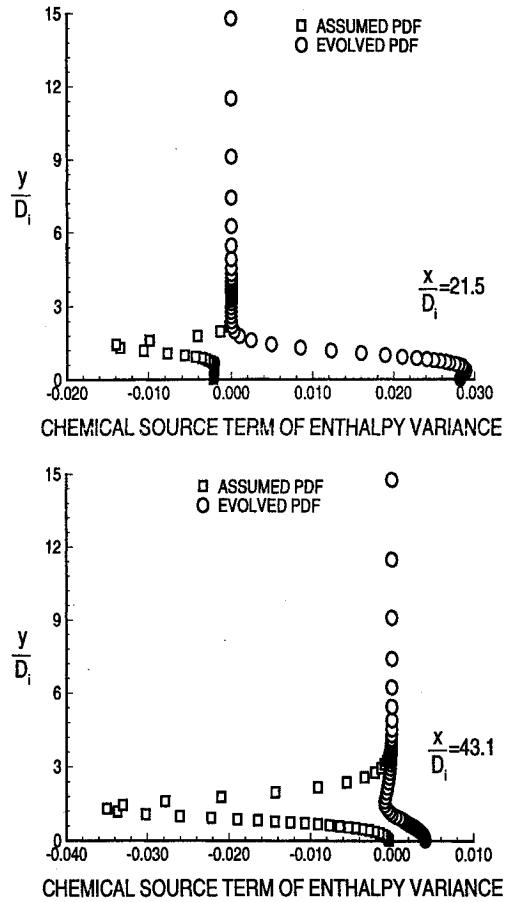

Fig. 10 Comparison of the chemical source term in the equation governing $\widetilde{h''^2}$.

Figure 8 compares the computed rms of the fluctuating component of temperature. At the 1-in. station (preceding combustion), the agreement of both sets of calculations with experiment is good, although the evolved PDF results show the variance to dissipate too rapidly in the outer jet region. Since the behavior of the mixing model is to deplete the variance,[5] this is an indicator that the model is overpredicting the mixing at the early stations. At the latter stations where combustion is taking place, neither approach agrees well with experiment. Similar statements can be made for the rms of the fluctuating component of the species mole fractions, some of which are shown in Ref. 12.

The sharp decline in the rms values of the scalars in regions of combustion for the assumed PDF calculations is a result of the strong dissipative nature of the chemical source terms in Eqs. (9) and (10). Figures 9 and 10 compare the values of these terms at the 2- and 4-in. stations with those computed by the evolved PDF. As is evident from these figures, the two solutions are showing quite different values for these quantities. The assumed PDF results show the chemical source term in Eq. (10) to act exclusively as a large dissipation term, whereas the evolved PDF results show much smaller values for this term that change sign through the flowfield. Previous assumed PDF calculations[21] using the same assumed PDF shown in Eq. (2), but without the inclusion of this chemical source term, showed much improved comparisons with experiment for the species variances. At that time, the accuracy of the higher-order correlations needed to compute this source term was questioned, since one would expect the correct shape of the PDF to have a stronger influence on the higher-order moments. These results strongly suggest this to be a correct assertion. The comparison of the chemical source term in Eq. (9) is shown in Fig. 10. Here, the assumed PDF calculations

yielded negative values exclusively, while the evolved PDF calculations yielded only positive values.

Concluding Remarks

The use of an evolution equation to compute the PDF in high-speed flows has not shown significant improvements over the simpler and cost efficient assumed PDF approach. The cost involved in solving the PDF evolution equation is quite high due mainly to the inclusion of a realistic kinetic model. There were several additional assumptions made in modeling the evolution PDF equation that are not required in modeling low-speed flows. These assumptions result from the inclusion of the dissipation and compressibility terms in the PDF equation, and the neglect of pressure fluctuations on the density. This last assumption prohibits the exact treatment of the chemical source terms which is the primary motivation for using the PDF approach. To remove this approximation, another thermodynamic variable must be brought into the PDF. Finally, the comparison of higher-order correlations showed large differences between the two approaches which suggests the assumed PDFs may be incapable of computing such terms with any reasonable degree of accuracy.

Acknowledgments

This work is supported in part by NASA Grant NAG-1-244 and the Mars Mission Research Center funded by NASA Grant NAGW-1331.

References

[1]Frankel, S. H., Drummond, J. P., and Hassan, H. A., "A Hybrid Reynolds Averaged/PDF Closure Model for Supersonic Turbulent Combustion," AIAA Paper 90-1573, June 1990.

[2]Narayan, J. R., and Girimaji, S. S., "Turbulent Reacting Flow Computations Including Turbulence-Chemistry Interactions," AIAA Paper 92-0342, Jan. 1992.

[3]Girimaji, S. S., "A Simple Recipe for Modeling Reaction-Rates in Flows with Turbulent Combustion," AIAA Paper 91-1792, June 1991.

[4]Baurle, R. A., Alexopoulos, G. A., Hassan, H. A., and Drummond, J. P., "An Assumed Joint-Beta PDF Approach for Supersonic Turbulent Combustion," AIAA Paper 92-3844, July 1992.

[5]Pope, S. B., "PDF Methods for Turbulent Reactive Flows," *Progress in Energy Combustion Science*, Vol. 11, Nos. 5, 6, 1985, pp. 119–192.

[6]Kollman, W., "The PDF Approach to Turbulent Flow," *Theoretical Computational Fluid Dynamics*, Vol. 1, No. 1, 1990, pp. 249–285.

[7]Hsu, A. T., "A Study of Hydrogen Diffusion Flames Using PDF Turbulence Model," AIAA Paper 91-1780, June 1991.

[8]Hsu, A. T., Tsai, Y. L. P., and Raju, M. S., "A PDF Approach for Compressible Turbulent Reacting Flows," AIAA Paper 93-0087, Jan. 1993.

[9]Hsu, A. T., Raju, M. S., and Norris, A. T., "Application of a PDF Method to Compressible Turbulent Reacting Flows," AIAA Paper 94-0781, Jan. 1994.

[10]Evans, J. S., Schexnayder, C. J., and Beach, H. L., "Application of a Two Dimensional Parabolic Computer Program to Prediction of Turbulent Reacting Flows," NASA TP 1169, March 1978.

[11]Cheng, T. S., Wehrmeyer, J. A., Pitz, R. W., Jarrett, O., Jr., and Northam, G. B., "Finite-Rate Chemistry Effects in a Mach 2 Reacting Flow," AIAA Paper 91-2320, June 1991.

[12]Baurle, R. A., Hsu, A. T., and Hassan, H. A., "Comparison of Assumed and Evolution PDF's in Supersonic Turbulent Combustion Calculations," AIAA Paper 94-3180, June 1994.

[13]Hsu, A. T., and Chen, J. Y., "A Continuous Mixing Model for PDF Simulations and Its Applications to Combusting Shear Flows," 8th Symposium on Turbulent Shear Flows, Munich, Germany, Sept. 1991.

[14]O'Brien, E. E., "The Probability Density Function (PDF) Approach to Reacting Turbulent Flows," *Turbulent Reacting Flows*, edited by P. A. Libby and F. A. Williams, Springer–Verlag, New York, 1980, pp. 185–218.

[15]Pope, S. B., "A Monte Carlo Method for the PDF Equations of Turbulent Reactive Flow," *Combustion Science and Technology*, Vol. 25, No. 2, 1980, pp. 159–174.

[16]Eklund, D. R., Drummond, J. P., and Hassan, H. A., "Numerical Modeling of Turbulent Supersonic Reacting Coaxial Jets," *AIAA Journal*, Vol. 28, No. 9, 1990, pp. 1633–1641.

[17]Jachimowski, C. J., "An Analytic Study of the Hydrogen-Air Reaction Mechanism with Application to Scramjet Combustion," NASA TP 2791, Feb. 1988.

[18]Cohen, L. S., and Guile, R. N., "Measurements in Freejet Mixing/Combustion Flows," *AIAA Journal*, Vol. 8, No. 6, June 1970, pp. 1633–1641.

[19]Baurle, R. A., Drummond, J. P., and Hassan, H. A., "An Assumed PDF Approach for the Calculation of Supersonic Mixing Layers," AIAA Paper 92-0182, Jan. 1992.

[20]Baurle, R. A., Alexopoulos, G. A., and Hassan, H. A., "Modeling of Supersonic Turbulent Combustion Using Assumed Probability Density Functions," *Journal of Propulsion and Power*, Vol. 10, No. 6, 1994, pp. 777–786.

[21]Baurle, R. A., Alexopoulos, G. A., and Hassan, H. A., "An Assumed Joint PDF Approach for Supersonic Turbulent Combustion," *Journal of Propulsion and Power*, Vol. 10, No. 4, 1994, pp. 473–485.